

## Supporting Information

### **Fabrication of iron manganese metal-organic framework derived magnetic MnFe<sub>2</sub>O<sub>4</sub>/C composites for broadband and highly efficient electromagnetic wave absorption**

Ruiwen Shu<sup>a,b\*</sup>, Jinling Zhang<sup>a</sup>, Shuai Liu<sup>a</sup> and Zaigang Luo<sup>a</sup>

*<sup>a</sup>School of Chemical Engineering, Anhui Provincial Key Laboratory of Specialty  
Polymers, Anhui University of Science and Technology, Huainan 232001, China*

*<sup>b</sup>Joint National-Local Engineering Research Centre for Safe and Precise Coal Mining,  
Anhui University of Science and Technology, Huainan 232001, China*

\*Corresponding Author:

Email: [rwshu@aust.edu.cn](mailto:rwshu@aust.edu.cn) (R. Shu).

## **Experimental section**

### **Characterization**

Crystalline structure was characterized by X-ray diffraction (XRD, LabX XRD-6000, Japan) with Cu-K $\alpha$  radiation ( $\lambda = 0.154$  nm) in the scattering range ( $2\theta$ ) of 5–80° at a scanning rate of 2°/min. Raman spectrum was acquired at room temperature by using a laser confocal Raman spectrometer (Renishaw-2000, UK) in the range of 1000–2000 cm<sup>-1</sup> with an excitation wavelength of 532 nm. The surface chemical composition and elemental valence were characterized by X-ray photoelectron spectroscopy (XPS, Thermo ESCALAB 250XI, USA). The magnetic properties were measured by vibrating sample magnetometer (VSM, Nanjing NanDa Instrument Plant HH-20, China) at room temperature. Micromorphology was observed with a field emission scanning electron microscopy (FESEM, GeminiSEM 500, Germany) and a field emission transmission electron microscopy (FETEM, FEI Tecnai G2 F20, USA) equipped with the energy dispersive spectrometer (EDS) device. The electrical conductivity was measured by a four-probe meter (Guangzhou Four Probe Technology Co., Ltd., RTS-8, China).

Electromagnetic parameters including the relative complex permittivity ( $\epsilon_r = \epsilon' - j\epsilon''$ ) and permeability ( $\mu_r = \mu' - j\mu''$ ) were acquired using the vector network analyzer (VNA, Keysight E5080B, USA) using the coaxial-line method in the frequency range of 2–18 GHz. The specimens were prepared by uniformly mixing the magnetic carbon composites with paraffin wax under a filling ratio of 30 wt.%, and then pressed the mixtures into a toroidal-shaped ring with an outer diameter of 7 mm, an inner diameter of 3.04 mm, and a thickness of approximately 2 mm.

### **Radar cross section (RCS) simulation**

The computer simulation technology (CST) Studio Suite 2018 was used to simulate the RCS in the far field response of an EMW absorber. A double-layer square model ( $100 \times 100 \text{ mm}^2$ ) is placed on the x-o-y plane, the bottom of which is made of the perfect electronic conductor (PEC), and an absorption layer is placed directly above the PEC (The thickness of PEC and absorption layer is 0.5 mm and 2.06 mm, respectively, at the frequency of 13.12 GHz). Among them, the detection angle is defined as  $\theta$ . The field monitoring frequency of each model is the frequency that corresponds to the composite material's minimum reflection loss ( $RL_{\min}$ ). There are no closed boundary conditions in any direction. Linearly polarized planar waves propagate along the z axis's negative direction, while electrically polarized waves propagate along the x axis's positive direction.<sup>2,3</sup> Furthermore, the scattering direction is determined by theta and phi in spherical coordinates, and the far-field response of the direction is calculated using the simulated sample's RCS, which can be defined by the following formula:<sup>1-3</sup>

$$\sigma (\text{dBm}^2) = 10 \log \left( \frac{4\pi S}{\lambda^2} \left| \frac{E_s}{E_i} \right| \right)^2 \quad (\text{S1})$$

Where  $S$ ,  $\lambda$ ,  $E_s$  and  $E_i$  denote the area of the simulation model, the wavelength of incident waves, the electrical field intensity of scattered waves and incident waves at the receiving position, respectively.

## Results and discussion

Fig. S1 displays the  $RL_{\min}$ , the thickness of absorber ( $t_m$ ) and  $|Z_{\text{in}}/Z_0|$  versus  $f$  curves of S2. The EMW absorption properties were further studied according to the quarter-wavelength ( $\lambda/4$ ) matching theory.<sup>4-6</sup> The relationship between the absorption peak frequency ( $f_m$ ) and  $t_m$  can be elucidated by  $\lambda/4$  matching theory as follows:<sup>7,8</sup>

$$t_m = \frac{n\lambda}{4} = \frac{nc}{4f_m \sqrt{|\epsilon_r \mu_r|}} \quad (n = 1, 3, 5, \dots) \quad (\text{S2})$$

If  $t_m$  and  $f_m$  satisfy the equation (S4), then the phase cancellation effect can effectively attenuate the incident waves.<sup>4-6</sup> It can be seen that as  $t_m$  increases, the  $RL$  peak of S2 shifts towards low frequencies. The pentagram signifies the experimental  $t_m$  (denoted as  $t_m^{\text{exp}}$ ). Remarkably, all the  $t_m^{\text{exp}}$  are exactly located at the  $\lambda/4$  curve, which reveals that the  $\lambda/4$  matching theory essentially determines the relationship between  $t_m$  and  $f_m$ . Therefore, the  $\lambda/4$  rule should be considered for designing high-performance EMW absorbers.

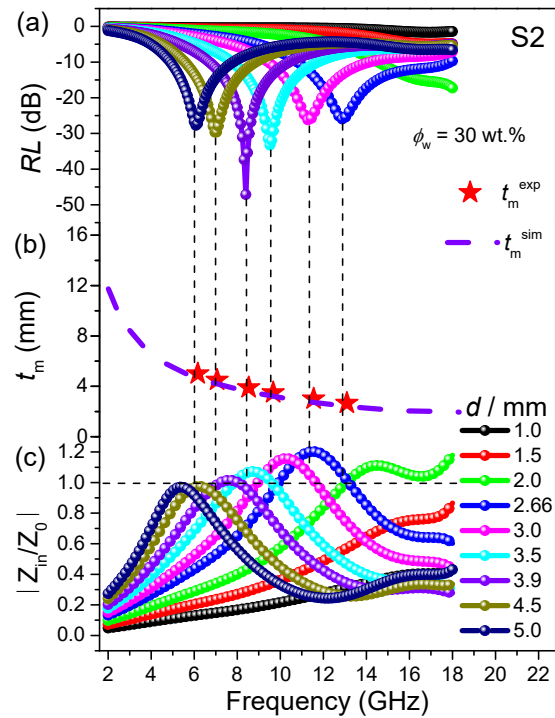


**Fig. S1**  $RL_{\min}$ ,  $t_m$  and  $|Z_{\text{in}}/Z_0|$  versus  $f$  curves of S2.

## References

- 1 X. Chen, Z. Wang, M. Zhou, Y. Zhao, S. Tang and G. Ji, *Chem. Eng. J.*, 2023, **452**, 139110.
- 2 R. Shu, Z. Zhao and X. Yang, *Chem. Eng. J.*, 2023, **473**, 145224.

- 3 H. Wang, H. Zhang, S. Feng, Y. Shi, H. Wang, K. Zhao, A. Nie, T. Li, M. Ma and Y. Ma, *J. Colloid Interf. Sci.*, 2023, **652**, 258-271.
- 4 X. Wang, L. Huang, T. Liu, F. Ding, Y. Li and Y. Yuan, *Compos. Part A-Appl. S.*, 2023, **173**, 107621.
- 5 X. Wang, J. Liao, R. Du, G. Wang, N. Tsidaeva and W. Wang, *J. Colloid Interf. Sci.*, 2021, **590**, 186-198.
- 6 P. Wang, J. Zhang, G. Wang, B. Duan, D. He, T. Wang and F. Li, *J. Mater. Sci. Technol.*, 2019, **35**, 1931-1939.
- 7 J. Yan, Y. Huang, Y. Yan, L. Ding and P. Liu, *ACS Appl. Mater. Interfaces*, 2019, **11**, 40781-40792.
- 8 P. Yi, X. Zhang, L. Jin, P. Chen, J. Tao, J. Zhou and Z. Yao, *Chem. Eng. J.*, 2022, **430**, 132879.